Hindawi
Advances in Astronomy
Volume 2022, Article ID 6672456, 10 pages
https://doi.org/10.1155/2022/6672456

Research Article

Testing Correspondence between Areas with Hydrated Minerals, as Observed by CRISM/MRO, and Spots of Enhanced Subsurface Water Content, as Found by DAN along the Traverse of Curiosity

M. V. Djachkova, I. G. Mitrofanov, S. Y. Nikiforov, D. I. Lisov, M. L. Litvak, and A. B. Sanin

Space Research Institute of the Russian Academy of Sciences, Moscow, Russia

Correspondence should be addressed to M. V. Djachkova; djachkova@np.cosmos.ru

Received 4 December 2020; Revised 16 February 2022; Accepted 19 March 2022; Published 1 April 2022

Academic Editor: Josep M. Trigo-Rodríguez

Possible correlation is studied between Water Equivalent Hydrogen (WEH) in the Martian subsurface, as measured by the DAN (Dynamic Albedo of Neutrons) instrument along the Curiosity traverse, and the presence of hydrated minerals on the surface, as seen from the orbit by CRISM (Compact Reconnaissance Imaging Spectrometer for Mars) instrument onboard MRO (Mars Reconnaissance Orbiter). Cross-analysis of the subsurface WEH values from DAN passive measurements with the distribution of hydrated minerals over the surface of Gale crater according to Specialized Browse Product Mosaics is performed for the initial 20 km part of traverse. As a result, we found an increase up to 0.4 wt% of the mean WEH value for the surface areas with the spectral signatures of polyhydrated sulfates. The increase is shown to be higher with the more prominent spectral signature on the surface. Similar WEH increase for the two other types of hydrated minerals, such as monohydrated sulfates and phyllosilicates, was not found for the tested part of the traverse. Polyhydrated sulfates being a part of the sedimentary deposits composing the surface of Gale crater should have considerable thickness that is necessary for the subsurface neutron sensing by DAN measurements.

1. Introduction

Gale crater was presumably formed during the late Noachian period (about 3.7-3.8 Ga) as a result of a large meteorite impact [1]. Its radius is about 150 km, and its initial depth is thought to be about 5 km. In its evolutional history from formation to the modern time, one may conditionally distinguish two main stages [2, 3]. The first stage corresponds to the Noachian period with a possibly warm and humid climate on the planet (or at least with episodic warm conditions), when Mars had a rather dense atmosphere. During this stage, the crater could be occasionally filled up with water and turned into a lake, at the bottom of which weathering of primary rocks in contact with an alkaline water environment produced phyllosilicates [4, 5]. The first stage ended by the beginning of Late Hesperian, when the climate of Mars became close to modern, with a thin atmosphere and a dry and cold surface. By the end of the first stage, Gale crater is thought to be filled up with layered sedimentary deposits [6].

In the second stage, the sedimentary deposits filling Gale crater were exposed, probably by wind erosion, creating Mount Sharp—5.5 km tall central mound which is not related to the central peak formed during the impact event [7]. The lowest visible units of Mount Sharp contain a variety of minerals that are indicative of aqueous conditions. Phyllosilicate (including the groups smectite, vermiculite, illite, kaolinite, serpentine, micas, and chlorite, commonly called clay minerals) spectral signatures are observed in some stratigraphic units near the base of

Mount Sharp, and sulfate-bearing minerals (such as anhydrite, bassanite, gypsum, and jarosite) are observed in younger, stratigraphically higher sedimentary units [8, 9]. This mineralogical transition suggests that the conditions under which the sediments were deposited changed through time. The broad mineral stratigraphy with sulfate-bearing units overlying phyllosilicate-bearing units has been recognized in similarly aged deposits globally on Mars [10]. This mineralogical succession may mark the beginning of the transition from Noachian to Hesperian, e.g., from a relatively wet and warm early Mars to a very dry and cold modern Mars [8, 11].

Thus, the sediments on the modern surface of Gale crater represent a natural record of Mars hydrological evolution, where a study of the composition and sequence of sedimentary strata from the crater floor up to the top of its central mound allows the disclosing of the changes of environmental conditions along the chronology of their formation [6]. At present, the ground water in the Martian soil may precipitate from the current thin atmosphere forming multilayers of molecules on the grains of regolith (as adsorbed water) and filling the porosity volume between grains (as free water ice). Though there is no direct evidence of ground ice, indirect evidence for the formation of frost at the surface of Gale crater exists [12]. Therefore, both kinds of water might exist currently in the shallow subsurface of Gale crater: water in the form of chemically bound molecules in hydrated minerals and water as adsorbed molecules in the regolith.

The presence of water in the subsurface of Gale crater is proved by the DAN active neutron sensing experiment onboard the Curiosity rover [13–15]. This paper presents the results of the comparative analysis of subsurface water abundance, as derived from DAN passive measurements data [16], together with data for the surface minerals distribution, as measured by CRISM onboard MRO. This analysis is thought to allow distinguishing which kind of ground water most likely exists in the subsurface along the Curiosity traverse over the bottom of Gale crater.

2. DAN Measurements along the Rover Traverse

The DAN instrument is an active neutron detector for sensing the subsurface layer of about 60 cm thickness by pulses of 14 MeV neutrons, produced by the pulsing neutron generator—PNG [15]. Pulses of neutrons produce the postpulse emission or *Dynamic Albedo of Neutrons*. Two DAN neutron counters record the time profiles of postpulse total neutron emission: CTN at thermal and epithermal energy range and CETN at epithermal energy range.

Since hydrogen in the Martian subsurface is most likely a part of either hydroxyl or water molecules, its content is conventionally measured in terms of Water Equivalent Hydrogen (WEH). On the other hand, the content of the neutron absorbing nuclei in the subsurface is evaluated by a single measurable parameter of the so-called Absorption Equivalent Chlorine—AEC [17]. Chlorine is selected because it is considered the major contributor to neutron absorption in the Martian regolith. The value of AEC takes into account not only the mass fraction of chlorine itself, but also all other absorbers in the subsurface matter, if their mass fractions differ from the values predicted by the so-called "standard composition" model of the Martian soil [18].

DAN started operating on Mars on August 12, 2012, just after the rover landing [19]. The data for the current analysis were obtained since that time until November 2018. That corresponds to 2218 sols and 19 971 m distance along the traverse. According to the rover flight rules, DAN active operations are only allowed at rover stops. Thus, estimates of WEH and AEC based on active measurements are available for the rover parking spots only [13]. For the first 20 km part of the rover traverse until sol 2218, the mean WEH and AEC values are found to be (2.6 ± 0.7) wt% and (1.0 ± 0.1) wt%, respectively [13].

While PNG operates only during active sessions lasting for 15–30 minutes at stops, DAN counters are working almost continuously, both at rover stops and during drives. When PNG is off, neutron counters continuously measure the local neutron emission. Flux and energy spectra of the surface albedo neutrons produced both by the Multi-Mission Radioisotope Thermoelectric Generator and Galactic Cosmic Rays largely depend on the presence of hydrogen, measured as WEH, and neutron absorbers, measured as AEC, in the subsurface matter. Thus, DAN continuous passive measurements give an opportunity to determine the WEH value at any particular spot below the rover along the traverse [16].

A special procedure of DAN passive data processing has been developed based on the empirically found relationships between active and passive data, measured simultaneously at the total number of 328 rover stops (see [16], for details). This empirical relationship, as well as the knowledge on the AEC, is used for obtaining the continuous profile of WEH values. The physical size of an individual spot on the surface for passive neutron sensing is shown to be about 3 meters in diameter [17], so the physical resolution of WEH variations along the traverse could be associated with such scale.

Distances between the rover stops vary from several meters up to hundreds of meters. To estimate AEC between two stops along the traverse, one needs to make an additional assumption for the scale of AEC spatial variations. It was suggested by [16], to use two approaches. The first one assumes a long-range (LR) scaling of AEC variability, when a smooth interpolation of AEC value is thought to be applicable along the path from one stop to another. In this case, the AEC value at each point between two stops could be derived from the interpolated values of active measurements at these stops. The second approach postulates that AEC might vary at a scale of several meters or so, presuming a short-range (SR) scaling of the AEC variability. In this case, the AEC value at each intermediate point of the traverse between two stops is thought to be randomly distributed according to the entire data set of the active measurements. For the part of the rover traverse studied in this paper, the mean AEC value for all active measurements is found to be equal to (1.0 ± 0.1) wt%.

After processing DAN passive data until sol 2218, two continuous profiles of the WEH spatial variability were obtained with a distance resolution of 3 meters using LR and/or SR approaches (Figure 1). The WEH value was found

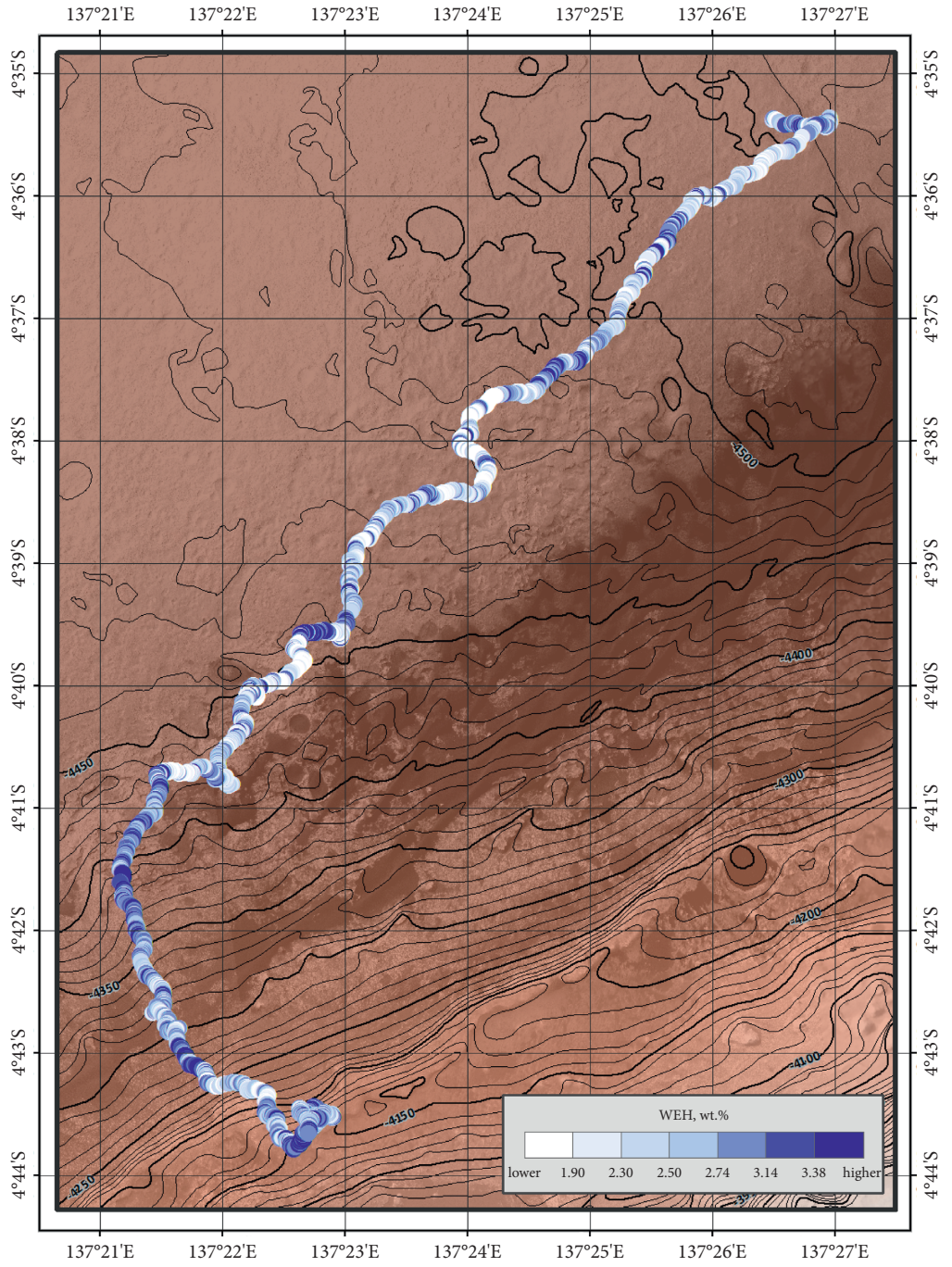

Figure 1: WEH as derived from DAN passive measurements using the LR approach for AEC variations along the Curiosity traverse.

to vary from around zero to 6.3 wt% [16]. These data were used for cross-analysis with CRISM spectral data products; see below.

3. CRISM Data Products for Cross-Analysis with DAN Data

CRISM instrument onboard the NASA MRO spacecraft performs imaging spectrometry in the visible and near-infrared wavelength range of 362–3920 nanometers. Such chemicals as iron, oxides, carbonates, etc. on the Martian surface have characteristic spectral features in the visible and infrared ranges and are distinguishable by CRISM [20].

For the current cross-analysis with DAN data, we used the publically available Specialized Browse Product Mosaics [21]. The CRISM team specifically created this data product for studying the Curiosity landing site. Hyperspectral images with high spatial resolution of about 20 m, not degraded by the increased noise or by atmosphere opacity, were selected as the source images for creating the products. Mathematical processing was applied to reflectance values at key wavelengths associated with diagnostic or indicative mineral

structure on the surface. The resulting composites of individual parameters reflect the thematic mineralogical diversity of the surface. A high value in the image plane indicates a relatively strong spectral feature for the particular product as compared to the range present regionally around the landing site [21].

In our study, two Specialized Browse Product Mosaic products were of special interest: "HYD" and "ALT." Both were constructed from images in the IR spectral range, as they characterize the spectral features of minerals that are thought to be formed by the interaction of rocks with liquid water. These two data products represent the surface distribution of such minerals as phyllosilicates (generally Fe-smectites) and mono- or polyhydrated Mg-sulfates (mostly kieserite and hexahydrite, respectively). The "HYD" data product shows indicators of hydrated minerals with a focus on the hydrated sulfates, while the "ALT" data product focuses on Fe/Mg phyllosilicates on the surface.

It should be taken into account that hydrated minerals, which are believed to be present in the shallow subsurface, might not be revealed by detection of their spectral indicators on the surface as they might be covered by dust or by a thin upper layer of some different mineralogical composition. While DAN senses the subsurface down to 1 m depth, CRISM images the uppermost layer of the Martian surface. However, the deposits of hydrated minerals that spread from the top down to the subsurface should be detectable by both instruments, CRISM from the orbit and DAN from the surface. To test the presence of such deposits and to map them along the rover, traverse was the goal of the performed cross-analysis, as presented below.

4. Cross-Analysis of DAN Passive Data with CRISM Data Products

The total number of 1028 CRISM mapping pixels, located along the traverse of the rover, was selected. For each such pixel with the size of about 20 meters, the mean WEH value was evaluated inside it according to the DAN passive measurements data, processed by the LR and SR approaches (see Section 3, Tables 1 and 2). Uncertainties of the WEH mean values were derived from the uncertainties of WEH values of the contributed distance intervals.

For each of the three types of hydrated minerals, such as phyllosilicates, monohydrated sulfates, and polyhydrated sulfates, the testing groups of corresponding CRISM pixels were selected, which manifest the spectral signatures of these minerals. Three groups with 51, 45, and 101 CRISM pixels were identified for phyllosilicates, monohydrated sulfates, and polyhydrated sulfate, respectively. The reference group of 831 CRISM pixels with no spectral signatures of any of the three types of hydrated minerals was also composed.

The method of cross-analysis of DAN and CRISM data is based on the comparison of the distribution of the mean WEH values for the testing group of CRISM pixels attributed to the particular testing mineral with the distribution of the mean WEH values for the reference group of CRISM pixels. As the simplest test, the average values and sample variances of WEH for the testing and the reference groups are compared. In addition, Pearson's chi-squared test is used for more precise testing of the statistical difference between them. Two distributions are thought to be statistically distinct, if the probability for their coincidence (p-level) is sufficiently small, $p < 0.001$.

One finds that there is no distinction of the distributions of WEH for groups of the CRISM pixels associated with either phyllosilicates or monohydrated sulfates from the reference group (Tables 1 and 2). For both cases of WEH estimation, using either LR or SR approach, the p-level values point out a rather good agreement between WEH distributions for testing and reference groups.

On the other hand, the evident effect of distinction from the reference group is found for the testing group of 101 CRISM pixels with the spectral signature of polyhydrated sulfates (Figure 2(a)). The differences between mean values of WEH are (0.2 ± 0.1) wt% for the LR approach (Table 1) and (0.4 ± 0.1) wt% for the SR approach (Table 2). According to Pearson's chi-squared test, the p-levels for the statistical coincidence between WEH distributions for the testing and reference groups are found to be much less than 0.001 (see Tables 1 and 2). Thus, the mean WEH value for the testing group of CRISM pixels, associated with the presence of polyhydrated sulfates, is confidently larger than the mean WEH value for the reference group of pixels, which do not have the spectral signature of such type of mineral.

It is reasonable to expect that the stronger spectral signature of the presence of minerals on the surface (seen as larger values in the RGB image plane) might correspond to a higher content of WEH detected by DAN in the subsurface. To check this assumption, the testing group of 101 CRISM pixels linked with polyhydrated sulfates was divided into two subgroups. The subgroup of "high intensity" includes pixels with the brightness >20 in the RGB image plane. Correspondingly, the subgroup of "low intensity" includes pixels with the brightness <20. The value of 20 was chosen as a dividing value for the total group into two statistically equal subgroups. For these two subgroups, the distributions of WEH were built, and their comparison with the reference distribution was performed (Tables 1 and 2).

Figure 3 shows the WEH distributions for the testing subgroups of CRISM pixels with "high intensity" polyhydrated sulfates for the cases of LR (a) and SR (b) approaches. The more pronounced shift to larger values is evident for the WEH distributions of "high intensity" subgroup in comparison with the WEH distribution for the reference group (Figure 3). Their mean WEH values become equal to (2.9 ± 0.1) wt% and (3.1 ± 0.1) wt% for the cases of LR and SR approaches, respectively. Besides, the Pearson test proves that WEH distributions for the "high intensity" subgroup of CRISM pixels are confidently distinct from the one for the reference group. The values of the p-level are much less than 0.001 (Tables 1 and 2).

As we stated in Section 2 of this paper, the value of WEH is not measured directly, but is obtained through the modelling of active and passive measurement data and is, therefore, model-dependent. To exclude the probable effects of model dependency, we performed the similar analysis as described above for the initial measured parameter of

Table 1: Comparison of parameters of WEH distributions for groups of CRISM pixels. WEH is derived from the DAN passive data for the case of long-range variability of AEC (LR case).

Groups of CRISM pixels		Coverage of the traverse (%)	Number of CRISM pixels	Number of DAN measurements	Mean of the WEH distribution (wt%)	Variance of the WEH distribution	χ^2 for Pearson criteria	p-level for Pearson criteria
Reference distribution		81	831	5467	2.54 ± 0.02	0.33	—	—
Phyllosilicates		5	51	293	2.57 ± 0.07	0.27	1.55	0.908
Monohydrated sulfates		4	45	307	2.41 ± 0.09	0.33	7.74	0.257
Polyhydrated sulfates	All	10	101	638	2.78 ± 0.05	0.25	24.30	0.0005
	Of "high intensity"	5	50	312	2.88 ± 0.07	0.24	21.79	0.0006
	Of "low intensity"	5	51	326	2.68 ± 0.07	0.24	7.81	0.252

Table 2: Comparison of parameters of WEH distributions for groups of CRISM pixels. WEH is derived from the DAN passive data for the case of short-range variability of AEC mass fraction (SR case).

Groups of CRISM pixels		Coverage of the traverse (%)	Number of CRISM pixels	Number of DAN measurements	Mean of the WEH distribution (wt%)	Variance of the WEH distribution	χ^2 for Pearson criteria	p-level for Pearson criteria
Reference distribution		81	831	5467	2.64 ± 0.02	0.30	—	—
Phyllosilicates		5	51	293	2.57 ± 0.06	0.17	18.46	0.001
Monohydrated sulfates		4	45	307	2.37 ± 0.09	0.33	11.04	0.051
Polyhydrated sulfates	All	10	101	638	3.06 ± 0.06	0.31	129.22	3.48×10^{-26}
	Of "high intensity"	5	50	312	3.10 ± 0.06	0.18	72.74	5.99×10^{-15}
	Of "low intensity"	5	51	326	2.75 ± 0.05	0.14	9.33	0.156

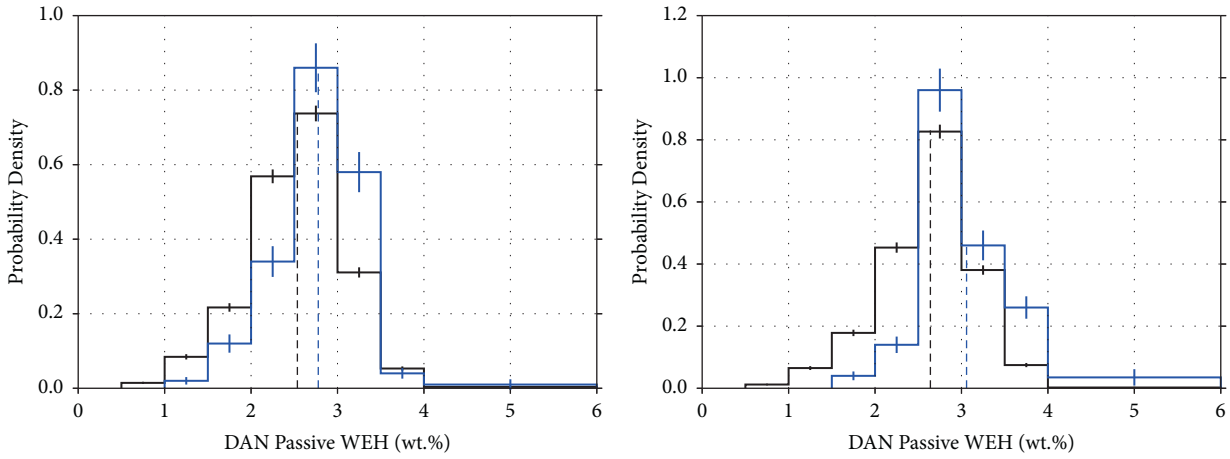

Figure 2: Distributions of the WEH values according to (a) LR approach and (b) SR approach for AEC estimations along the Curiosity traverse. The black line shows WEH distribution for the reference group of the CRISM pixels, which do not have signatures of hydrated minerals. The blue line represents the WEH distribution for the group of CRISM pixels with the spectral signature of polyhydrated sulfates. Dotted lines indicate the mean WEH values of the distributions.

neutron emission. Instead of the WEH value, we used the ratio of the count rates of total C_{CTN} and epithermal C_{CETN} neutrons emitted by the surface, namely, $F_{DAN} = C_{CTN}/C_{CETN}$ (for more details, see [16]). The results of the performed analysis are described in Table 3. The relationship between the parameters of the F_{DAN} distributions is found to be similar to the same parameters of the WEH distributions (Tables 1 and 2). Only the distribution of F_{DAN} for the testing group of CRISM pixels associated with the presence of polyhydrated sulfates is confidently different from the reference distribution of F_{DAN} for the group of pixels, which do not have the spectral signature of hydrated minerals. So, one

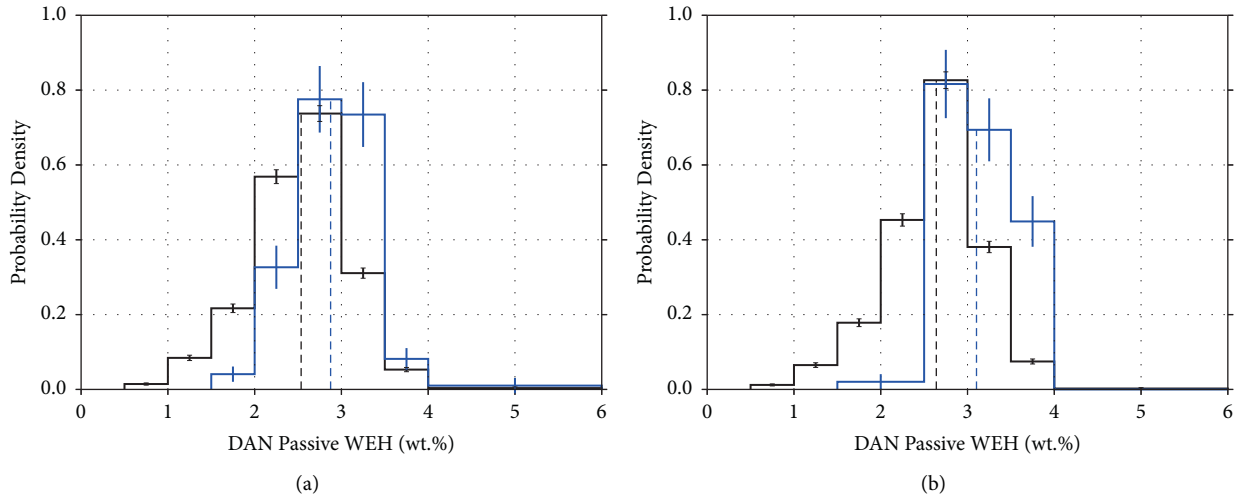

Figure 3: Same as for Figure 2, but the blue line represents the WEH distribution for the group of CRISM pixels with the "high intensity" spectral signature of polyhydrated sulfates.

Table 3: Comparison of parameters of F_{DAN} distributions for groups of CRISM pixels.

Groups of CRISM pixels		Coverage of the traverse (%)	Number of CRISM pixels	Number of DAN measurements	Mean of the F_{DAN} distribution	Variance of the F_{DAN} distribution	χ^2 for Pearson criteria	p-level for Pearson criteria
Reference distribution		81	831	5467	3.20 ± 0.02	0.26	—	—
Phyllosilicates		5	51	293	3.13 ± 0.05	0.14	7.74	0.052
Monohydrated sulfates		4	45	307	2.95 ± 0.08	0.28	11.12	0.049
Polyhydrated sulfates	All	10	101	638	3.47 ± 0.04	0.16	34.56	5.71×10^{-7}
	Of "high intensity"	5	50	312	3.63 ± 0.06	0.16	53.69	1.31×10^{-11}
	Of "low intensity"	5	51	326	3.31 ± 0.05	0.12	8.70	0.034

had to conclude that the relationship found between the presence of polyhydrated sulfates and increase of water in the shallow subsurface is not produced by WEH deconvolution procedure, but manifests physical relation between such minerals and neutron emission.

5. Discussion

Thus, the conclusion should be drawn that, along the traverse from the landing site to the distance mark of about 20 km, the presence of polyhydrated sulfates on the surface, as observed by CRISM, is consistent with the increase of WEH values within a subsurface layer of about 60 cm thickness, as measured by DAN. On the other hand, no such phenomenon is found for another group of CRISM pixels associated with the spectral signatures of phyllosilicates or monohydrated sulfates. One may speculate that the part of the traverse, which manifests the phenomenon of CRISM-DAN cross-correspondence, is associated with the sedimentary strata containing polyhydrated sulfates probably with significant thickness that leads to enhanced mass fraction of water in comparison with the "usual" subsurface with some standard mass fraction of water. The top surfaces of such matter are observable by CRISM from the Martian orbit and their deeper volumes are detectable by DAN from the Martian surface. One suggests naming such strata as layers of polyhydrated sulfates-rich matter, or PHSR matter.

To test this simplest interpretation of the found phenomenon, one might check the possibility that the observed WEH distribution in the area with PHSR matter (Figure 2) could be modeled by a bimodal function with two distinct components: the "less-WEH" component and "more-WEH" component (Figure 4). The "less-WEH" component could be associated with the "usual" matter. Its shape could be taken from the known distribution of WEH for the reference group of CRISM pixels with no signatures of any of the three types of hydrated minerals (Figure 2). The mean values for WEH of this component are known to be equal to (2.54 ± 0.02) wt% for the LR approach and (2.40 ± 0.02) wt% for the SR approach (see Table 1). The "more-WEH" component could be associated with polyhydrated sulfates. As the simplest option, this "more-WEH" component could be represented by a normal distribution with two free parameters: the mean value and the sample variance.

Using such a bimodal model, one may try to fit the observed WEH distribution in the area of CRISM pixels with a spectral signature of polyhydrated sulfates. In addition to the two free parameters of the "more-WEH" component, one more parameter should be used for fitting: the relative fraction α of this component with respect to the total integral

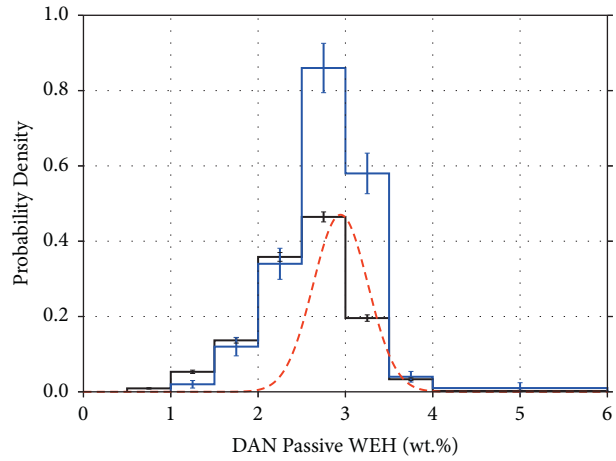

Figure 4: The bimodal distribution of WEH for the pixels with the spectral signature of polyhydrated sulfates (blue line): the more-WEH component of the distribution (dotted red line) represents the surface, dominated by polyhydrated sulfates, the less-WEH component of the distribution (black line) is the reference distribution taken with its modelled contribution.

of the entire observed distribution. Two cases of the observed distributions are tested for WEH derived by either LR or SR approaches of DAN passive data processing. One-tailed Pearson's chi-squared test is applied for finding the best fitting parameters of the bimodal model (Table 4).

In both cases, for LR and SR approaches, the Pearson criteria give very good p-level values for consistency between the observed distribution and the modeling function; i.e., it is between 0.001 and 0.15 (Table 4). The "more-WEH" component has the mean WEH values equal to 3.0 or 3.6 wt % for the cases of LR and SR, respectively (Table 4 and Figure 2).

Taking into account this result, one may speculate that the two components of WEH distribution represent two fractions of PHSR matter. The "less-WEH" component corresponds to the "usual" soil and the "more-WEH" component might be attributed to deposits of polyhydrated sulfates. The bimodal approximation of the observed WEH distribution for the area of PHSR matter allows determining the fraction parameter α for the contribution of "more-WEH" component. This fraction is about 0.37 or 0.12 (as a part of 1) of the entire WEH distributions, based on either LR or SR approaches, respectively. In the case of the proposed identification, such a fraction α corresponds to the part of the subsurface volume, which contains deposits of polyhydrated sulfates with the thickness large enough for neutron sensing. Another fraction $(1-\alpha)$ corresponds to the "usual" soil. Interestingly, the fraction of the "more-WEH" component is approaching the value of 1 for the subgroup of 51 pixels of "high intensity" spectral signature of polyhydrated sulfates (Table 4). It is another piece of evidence for the identification of "more-WEH" component in the areas, the substances of which is the deposition of polyhydrated sulfates.

The fraction of "usual" soil in the PHSR matter might exist practically everywhere along the traverse. This substance does not contain noticeable quantities of any of the three types of hydrated minerals and has an average WEH of about 2.5 wt% (see Tables 1 and 2). The WEH value for this second fraction of PHSR matter corresponds to the number of water molecules in the structure of polyhydrated sulfates. Its value was derived from the DAN data, as about 3 wt% (Table 4). The chemically bound water of hydrated minerals was embedded in their structure long time ago, when these minerals were formed in the aqueous conditions. Therefore, the type of PHS-dominated substance is thought to contain the "initial water" of Mars.

The mass fraction of polyhydrated sulfates in the subsurface substance may vary along the traverse. At some spots with the most intense spectral signatures of polyhydrated sulfates, the "more-WEH" component, as shown above, may contribute the observed WEH distribution entirely. One may use the DAN passive data for testing the presence of polyhydrated sulfates in the subsurface along the traverse with the spatial resolution about hundreds meters or so.

For performing such test we split the total path of about 20 km into 132 distance intervals of 150 meters long, each including around 50 passive measurements of WEH with a spatial resolution of 3 meters. The distribution of the WEH values for each distance interval is tested by the already known bimodal function with only one variable parameter α, as the fractionation of the already known components of "less-water" and "more-water," α and $1-\alpha$, respectively. The best fitting value of α could be considered as the average mass fraction of polyhydrated sulfates in the subsurface. Performing such an analysis for all 132 distance intervals, one obtains the profile of the polyhydrated sulfates mass fraction along the traverse (Figure 5).

The profile shows that the highest value of α equal to 0.21 (the confidence is 15%) is observed at the area around a distance mark of 16,300 m. Indeed, according to the CRISM data, this area is characterized by the increased value of the spectral signature brightness for polyhydrated sulfates (Figure 6). Thus, the analysis of the DAN passive data made it possible to identify sites with an increased content of polyhydrated sulfates in the shallow subsurface. One of such sites is found at the distance mark of 16,300 meters of the traverse on the way from Bagnold Dunes to Vera Rubin ridge.

Table 4: Best fitting parameters of bimodal model for WEH distribution for the group of CRISM pixels with the signature of polyhydrated sulfates (cases of LR and SR are presented for estimations of WEH from the DAN passive data).

Distributions of WEH for CRISM pixels along the rover traverse		Fraction of the component of bimodal model representing polyhydrated sulfates (in parts of 1)	Parameters of the normal distribution of WEH for the component of bimodal model representing polyhydrated sulfates		χ^2 minimum value	p-level
			Mean (wt %)	Variance		
Polyhydrated sulfates	According to the LR case	0.37 (+0.11/−0.10)	3.00	0.24	6.75	0.150
Polyhydrated sulfates of "high intensity"		0.99 (+0.01/−0.64)	2.87	0.43	8.78	0.032
Polyhydrated sulfates	According to the SR case	0.12 (+0.01/−0.01)	3.59	0.19	17.29	0.001
Polyhydrated sulfates of "high intensity"		1.00 (+0.00/−0.21)	3.13	0.22	5.64	0.060

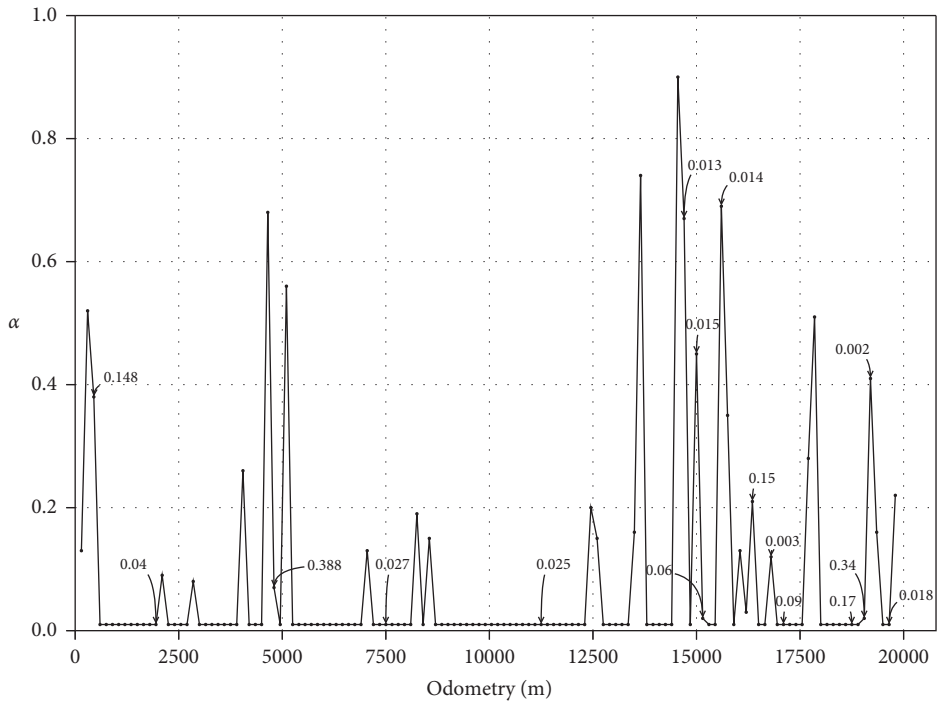

Figure 5: The distance profile of the polyhydrated sulfates mass fraction (α) along the traverse. The captions correspond to the significant probabilities of α.

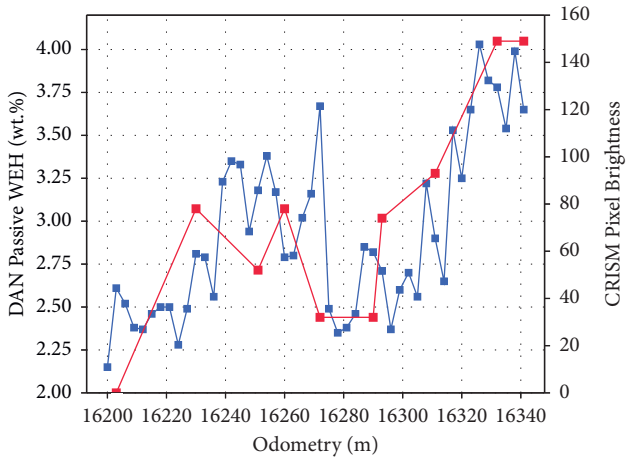

Figure 6: The distance profile of the DAN passive measurements of WEH with spatial resolution of 3 m (blue line) and the pixel brightness corresponding to polyhydrated sulfates according to CRISM specialized browse product mosaics (red line) for the distance interval of 16,200–16,350 m. The dotted line shows the mean WEH value for the whole traverse.

6. Conclusions

The cross-analysis of the WEH values from the DAN passive measurements onboard Curiosity and Specialized Browse Product Mosaics of CRISM spectrometer onboard the MRO was performed for the part of the rover traverse from the landing site up to the distance mark 19 971 m. It was found that traverse intervals with the spectral signature of polyhydrated sulfates, as detected by CRISM, contain more WEH in the subsurface in comparison with the intervals that do not manifest signatures of any of the three selected types of hydrated minerals, such as phyllosilicates and mono- and polyhydrated sulfates. This effect points out that polyhydrated sulfates exist at some places along the traverse, as layers with up to 60 cm thickness that are well detectable by DAN with its sensing depth of about 60 cm in the subsurface.

The bimodal distribution of WEH was found for such distance intervals along the traverse with the spectral signature of polyhydrated sulfates. The "less-WEH" component of this distribution is consistent with the distribution observed at the dominating majority of distance intervals that do not manifest any spectral signatures of all three tested types of hydrated minerals. The average water content for this type of matter is 2.5 wt%. The "more-WEH" component of this distribution is thought to be associated with the second type of matter, whose composition is likely dominated by polyhydrated sulfates component. The value of WEH for this type is about 3 wt% or larger.

The absence of any difference between WEH distributions for the distance intervals without spectral signatures of the three tested types of hydrated minerals and for distance intervals with spectral signatures of phyllosilicates and monohydrated sulfates does not necessarily make a discrepancy between CRISM and DAN observations. Indeed, the uppermost layer of the subsurface with such hydrated minerals may be seen by CRISM, but might be too thin for the detection by DAN. One may suspect that for some reason the top layers with polyhydrated sulfates are thick enough for being detected by DAN, while the top layers of phyllosilicates and monohydrated sulfates are not.

The CRISM pixels with the spectral signature of polyhydrated sulfates cover about 10% of the 20 km long rover traverse that was analyzed. The fact of the large thickness of polyhydrated sulfates deposits suggests a long period of time in the past, when such layer had enough time to be accumulated. On the other hand, the areas of CRISM pixels with spectral signatures of phyllosilicates and monohydrated sulfates are most likely associated with rather thin layers on top of the ordinary rocks and soil. DAN is not sensitive to the presence of such thin layers on top of the ordinary matter. One may expect that the presence of such hydrated minerals will also be proved by cross-analysis of CRISM and DAN data, when the rover climbs up Aeolis Mons, where the deposits if phyllosilicates or monohydrated sulfates might be thick enough for the detection of the WEH increase contributed by them.

Data Availability

Data from this work are publicly accessible on the Planetary Data System, https://www.pds.nasa.gov/.

Disclosure

This paper was presented at EGU General Assembly 2020 [22].

Conflicts of Interest

The authors declare that they have no conflicts of interest.

Acknowledgments

This work was funded by the Ministry of Science and Higher Education of the Russian Federation, "Exploration" theme grant AAAA-A18-118012290370-6. The authors highly appreciate the excellent support of the DAN investigation from the Curiosity project team.

References

[1] B. J. Thomson, N. T. Bridges, R. Milliken et al., "Constraints on the origin and evolution of the layered mound in Gale Crater, Mars using Mars Reconnaissance Orbiter data," *Icarus*, vol. 214, no. 2, pp. 413–432, 2011.

[2] N. A. Cabrol, E. A. Grin, H. E. Newsom, R. Landheim, and C. P. McKay, "Hydrogeologic evolution of gale crater and its relevance to the exobiological exploration of mars," *Icarus*, vol. 139, no. 2, pp. 235–245, 1999.

[3] S. Clifford and T. J. Parker, "The evolution of the martian hydrosphere: implications for the fate of a primordial ocean and the current state of the northern plains," *Icarus*, vol. 154, no. 1, pp. 40–79, 2001.

[4] O. Abramov and D. A. Kring, "Impact-induced hydrothermal activity on early Mars," *Journal of Geophysical Research*, vol. 110, Article ID E12S09, 2005.

[5] S. P. Schwenzer, O. Abramov, C. C. Allen et al., "Gale crater: formation and post-impact hydrous environments," *Planetary and Space Science*, vol. 70, no. 1, pp. 84–95, 2012.

[6] J. P. Grotzinger, S. Gupta, M. C. Malin et al., "Deposition, exhumation, and paleoclimate of an ancient lake deposit, gale crater, mars," *Science*, vol. 350, no. 6257, Article ID aac7575, 2015.

[7] R. Y. Sheppard, R. E. Milliken, M. Parente, and Y. Itoh, "Updated perspectives and hypotheses on the mineralogy of lower Mt. Sharp, Mars, as seen from orbit," *Journal of Geophysical Research: Planets*, vol. 126, no. 2, Article ID e2020JE006372, 2021.

[8] R. E. Milliken, J. P. Grotzinger, and B. J. Thomson, "Paleoclimate of mars as captured by the stratigraphic record in gale crater," *Geophysical Research Letters*, vol. 37, Article ID L04201, 2010.

[9] E. B. Rampe, D. F. Blake, T. F. Bristow et al., "Mineralogy and geochemistry of sedimentary rocks and eolian sediments in gale crater, mars: a review after six earth years of exploration with curiosity," *Geochemistry*, vol. 80, no. 2, Article ID 125605, 2020.

[10] J. P. Grotzinger and R. E. Milliken, "The sedimentary rock record of Mars: distribution, origins, and global stratigraphy," *SEPM Special Publications*, vol. 102, pp. 1–48, 2012.

[11] J.-P. Bibring, Y. Langevin, J. F. Mustard et al., "Global mineralogical and aqueous mars history derived from OMEGA/mars express data," *Science*, vol. 312, no. 5772, pp. 400–404, 2006.

[12] G. M. Martínez, E. Fischera, N. O. Rennó et al., "Likely frost events at Gale crater: analysis from MSL/REMS measurements," *Icarus*, vol. 280, pp. 93–102, 2016.

[13] D. I. Lisov, M. L. Litvak, A. S. Kozyrev, I. G. Mitrofanov, and A. B. Sanin, "Data processing results for the active neutron measurements by the DAN instrument on the curiosity mars rover," *Astronomy Letters*, vol. 44, no. 7, pp. 482–489, 2018.

[14] M. L. Litvak, I. G. Mitrofanov, A. B. Sanin et al., "Local variations of bulk hydrogen and chlorine-equivalent neutron absorption content measured at the contact between the sheepbed and Gillespie Lake units in Yellowknife Bay, gale crater, using the DAN instrument onboard curiosity," *Journal of Geophysical Research: Planets*, vol. 119, no. 6, pp. 1259–1275, 2014.

[15] I. G. Mitrofanov, M. L. Litvak, A. B. Varenikov et al., "Dynamic albedo of neutrons (DAN) experiment onboard NASA's mars science laboratory," *Mars Science Laboratory*, vol. 170, no. 1–4, pp. 559–582, 2012.

[16] S. Y. Nikiforov, I. G. Mitrofanov, M. L. Litvak et al., "Assessment of water content in martian subsurface along the traverse of the curiosity rover based on passive measurements of the DAN instrument," *Icarus*, vol. 346, Article ID 113818, 2020.

[17] A. B. Sanin, I. G. Mitrofanov, M. L. Litvak et al., "Data processing of the active neutron experiment DAN for a Martian regolith investigation," *Nuclear Instruments and Methods in Physics Research Section A: Accelerators, Spectrometers, Detectors and Associated Equipment*, vol. 789, pp. 114–127, 2015.

[18] J. Bell, Ed., *The Martian Surface. Composition, Mineralogy and Physical Properties*, Cambridge University Press, Cambridge, NY, USA, 2008.

[19] I. G. Mitrofanov, M. L. Litvak, A. B. Sanin et al., "Water and chlorine content in the Martian soil along the first 1900 m of the curiosity rover traverse as estimated by the DAN instrument," *Journal of Geophysical Research*, vol. 119, no. 7, pp. 1579–1596, 2014.

[20] S. Murchie, R. Arvidson, P. Bedini et al., "Compact reconnaissance imaging spectrometer for mars (CRISM) on mars reconnaissance orbiter (MRO)," *Journal of Geophysical Research*, vol. 112, no. E5, 2007.

[21] CRISM, "Description of specialized browse product mosaics," 2020, http://crism.jhuapl.edu/msl_landing_sites/index_news.php.

[22] M. Djachkova, I. Mitrofanov, M. Litvak, D. Lisov, S. Nikiforov, and A. Sanin, "Testing correspondence between areas with hydrated minerals, as observed by CRISM onboard MRO, and spots of enhanced subsurface water content, as found by DAN along the traverse of curiosity," *EGU General Assembly*, Article ID EGU2020-9993, 2020.